Published in "Research on Chemical Intermediates 41(4): 1881–1891, 2015"
which should be cited to refer to this work.

Synthesis, X-ray structure and DFT calculation of oxido-vanadium(V) complex with a tridentate Schiff base ligand

Iran Sheikhshoaie · S. Yousef Ebrahimipour · Aurelien Crochet · Katharina M. Fromm

Abstract Reaction of 4-bromo-2-(((5-chloro-2-hydroxyphenyl) imino)methyl) phenol (H_2L) with $VOSO_4 \cdot XH_2O$ generates the oxido-vanadium(V) complex $[VOL(OCH_3)(OHCH_3)]$, that characterized by FT-IR, UV–Vis, and elemental analysis. The complex was also characterized by single crystal X-ray diffraction crystallography. A DFT calculation was carried out on the complex using the B3LYP/6-31+G(d,p) method. The agreement between the theoretical and experimental data is good. NBO data shows that the donation from donor atoms to the metal center is greater than back bonding.

Keywords V(V) complex · DFT · X-ray crystal structure · NBO · Schiff base

Introduction

The synthesis, characterization, and coordination chemistry of vanadium(V) Schiff base complexes have undergone noticeable development in recent decades due to the various interesting properties of these complexes [1–3]. Vanadium(V) complexes have a significant role in many catalytic and inhibitory biological processes [4, 5].

Electronic supplementary material

I. Sheikhshoaie (✉) · S. Y. Ebrahimipour (✉)
Department of Chemistry, Shahid Bahonar University, 76175-133 Kerman, Iran
e-mail: i_shoaie@yahoo.com

A. Crochet
FriMat, University of Fribourg, Chemin du Musée 6, 1700 Fribourg, Switzerland

K. M. Fromm
Department of Chemistry, University of Fribourg, Chemin du Musée 9, 1700 Fribourg, Switzerland

Many simple vanadium salts show only a small degree of absorption by tissues and have side effects, but the toxicity of vanadium complexes, especially those containing the vanadyl moiety, is much less, and these vanadium complexes are more readily absorbed by the tissues [6]. The insulin mimics properties and especially its role in diabetes type 1 and 2, and its anti-tumor properties are the other aspects of the biochemical involvement of vanadium [7, 8]. The ability of vanadium compounds to affect DNA cleavage has led to their use in anti-cancer applications [9].

In recent years, DFT calculation is one of the attractive useful methods that have determined vague aspects of physicochemical properties of transition metal complexes [10–14].

Herein, we report the synthesis, spectroscopy, X-ray structural and DFT studies of V(V) complex [VOL(OCH_3)($OHCH_3$)] with 4-bromo-2-(((5-chloro-2-hydroxyphenyl)imino)methyl)phenol (H_2L) as a tridentate Schiff base ligand.

Experimental

Materials and instrumentation

All chemicals and solvents used were of analytical reagent grade and were used as received. The ligand H_2L was prepared according to the reported procedure [15]. Micro-analyses were determined on a Heracuse CHN rapid analyzer. The IR spectra was measured as KBr pellets on a FT-IR 8400-SHIMADZU spectrophotometer (400–4,000 cm^{-1}). The electronic spectrum was recorded in MeOH on a Shimadzu 160 spectrophotometer. Melting point was determined on a Gallenkamp melting point apparatus.

The crystal was mounted on a loop and all geometric and intensity data were taken from a single crystal. Data collection using Mo-K_α radiation ($\lambda = 0.71073$ Å) was performed at 200 K with a STOE IPDS II diffractometer equipped with an Oxford Cryosystem open flow cryostat.

Synthesis of [VOL(OCH_3)($OHCH_3$)]

The H_2L (0.1 mmol) was dissolved in CH_3CN (5 ml). $VOSO_4{\cdot}XH_2O$ (0.1 mmol) was added to the ligand solution and gently refluxed for 1 h. After cooling, the resulting solid was filtered off, washed with cold absolute ethanol, and dried in a desiccator over anhydrous $CaCl_2$. Red crystals were obtained by recrystallization from methanol/ethanol (50:50 v/v).

Yield: 0.033 g, 73 %. m.p.: 235 °C. Anal. Calc. for $C_{15}H_{14}BrClNO_5V$ (454.57 g mol^{-1}): C, 39.63; H, 3.10; N, 3.08. Found: C, 39.88; H, 3.21; N, 3.41 %. IR (KBr), cm^{-1}: ν(C=N) 1,604 s, ν(V=O) 964 s. UV/Vis (MeOH), λ_{max}, nm (ε, M^{-1} cm^{-1}): 245(64,565), 272(42,480), 441(23,442).

Crystal structure determination

The structure was solved and refined using full-matrix least-squares on F^2 with the SHELX-97 package [16]. All heavy atoms were refined anisotropically. H4 of the

Table 1 Crystal data and structure refinement for [VOL(OCH_3)($OHCH_3$)]

Empirical formula	C15 H14 Br Cl NO5V	
Formula weight	454.57	
Temperature	200 (2) K	
Wavelength	0.71073 Å	
Crystal system	Monoclinic	
Space group	$P\ 2_1/n$	
Unit cell dimensions	$a = 10.1007\ (7)$ Å	$\alpha = 90°$
	$b = 9.8800\ (4)$ Å	$\beta = 100.495(5)°$
	$c = 17.3786\ (11)$ Å	$\gamma = 90°$
Volume	1,705.28 (17) $Å^3$	
Z	4	
Density (calculated)	1.771 Mg/m^3	
Absorption coefficient	3.106 mm^{-1}	
$F(000)$	904	
Crystal size	$0.400 \times 0.287 \times 0.140\ mm^3$	
Theta range for data collection	2.18–25.00°	
Index ranges	$-12 \leq h \leq 12, -11 \leq k \leq 11, -20 \leq l \leq 20$	
Reflections collected	31,458	
Independent reflections	2,993 [R(int) = 0.0407]	
Completeness to theta = 25.00°	100.0 %	
Absorption correction	Integration	
Max. and min. transmission	0.1580 and 0.0791	
Refinement method	Full-matrix least-squares on F^2	
Data/restraints/parameters	2,993/1/222	
Goodness-of-fit on F^2	1.065	
Final R indices [$I > 2$ sigma(I)]	$R1 = 0.0280$, w$R2 = 0.0741$	
R indices (all data)	$R1 = 0.0342$, w$R2 = 0.0762$	
Largest diff. peak and hole	0.602 and −0.708 e. $Å^{-3}$	

OH group was located on an electron difference map and freely refined. The remaining H atoms were positioned geometrically and allowed to ride on their parent atoms, with C–H = 0.95–1.00 Å and U_{iso}(H) = 1.2 times U_{eq}(C). Table 1 shows the crystallographic data and details of the structure analysis.

Computational details

All calculations were performed with the GAUSSIAN 03 package [17], using the B3LYP exchange correlation function [18, 19]. The geometry of the complex was fully optimized in the gas phase using the B3LYP/6-31+G(d,p) basis set for H, C, N, O, Cl, and Br atoms and the LanL2DZ basis set for vanadium without any symmetry constraint. The frequency calculations were performed at the same level and the lack of imaginary frequencies provided evidence for full optimization of the

structure. Natural bond orbital (NBO) calculations were performed with the NBO code included in GAUSSIAN03. GaussSum 2.2 was used for analyzing the molecular orbitals [20].

Results and discussion

Characterization

According to our previous work [15], in solution, the H_2L exists in the *enol* tautomeric form (Scheme 1). The non-observation of the ν (NH) band, present in the ligands at 3,130 cm^{-1}, indicates the *enol* form of ligand used upon coordination to the V(V) center. A band at 1,297 cm^{-1} is due to the stretching vibration of C–O that shows a red shift with respect to the free ligand, indicating coordination occurred of the deprotonated phenolic OH atom [21].

The 23 cm^{-1} shift of the azomethine band towards lower frequency on complexation with the metal suggests coordination to the metal ion through an imine nitrogen atom [22]. The *ν*(V=O) band of the vanadyl moiety was observed at 964 cm^{-1} [23].

For the V(V) complex, two bands at 245 and 272 nm in UV–Vis spectrum are attributed to intraligand $\pi \rightarrow \pi^*$ transition [24]. The lowest energy transition band is observed near 441 nm, which is attributed to a LMCT charge transfer from a *p*-orbital on the lone-pair of the ligand oxygen atoms to the empty *d*-orbital of the vanadium atom [25].

Crystal structure of V(V) complex

Ortep representation and unit cell for V(V) complex are shown in Fig. 1, and selected bond length and angles are listed in Table 2.

As it can be seen, [VOL(OCH_3)($OHCH_3$)] crystallizes in the monoclinic $P\ 2_1/n$ space group with unit cell parameters, $a = 10.1007(7)$ Å, $b = 9.8800(4)$ Å, $c = 17.3786(11)$ Å, and $\beta = 100.495(5)°$, with $Z = 4$. The complex has the expected octahedral geometry around the central metal. In [VOL(OCH_3)(OH CH_3)], the ONO tridentate ligand is in the meridional position, and the methoxy group and

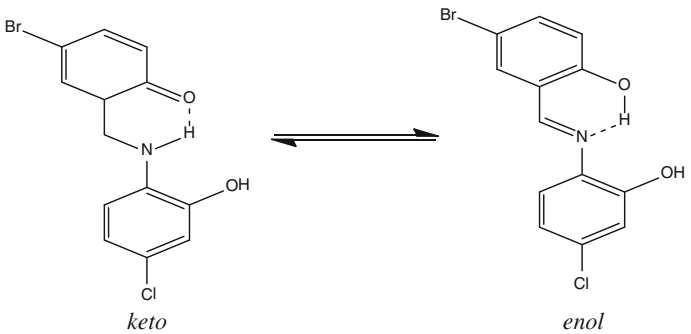

Scheme 1 The tautomeric forms of the free ligand (H_2L)

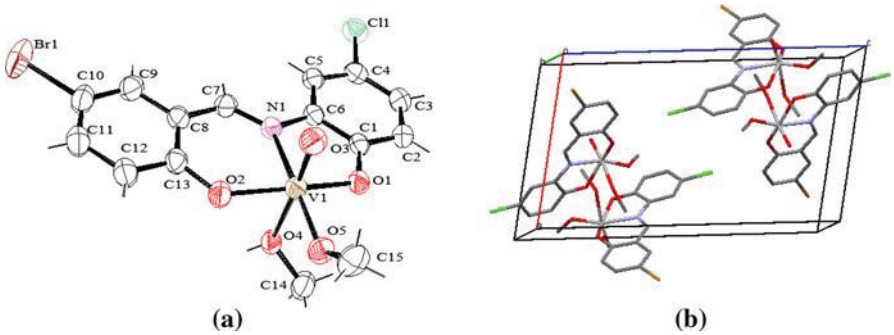

Fig. 1 **a** Molecular structure of V(V) complex with the crystallographic numbering scheme adopted. Displacement ellipsoids are drawn at the 50 % probability level. **b** Unit cell of the complex

Table 2 Selected calculated and experimental bond lengths (Å) and bond angles (°) for [VOL(OCH_3)($OHCH_3$)]

Bond lengths	Exp.	B3LYP/ 6-31 + G	Bond angles	Exp.	B3LYP/ 6-31 + G
Br(1)–C(10)	1.906(3)	1.906	O(3)–V(1)–O(5)	101.74(9)	103.13
V(1)–O(3)	1.588(2)	1.574	O(3)–V(1)–O(2)	100.07(9)	101.27
V(1)–O(5)	1.759(2)	1.769	O(5)–V(1)–O(2)	100.31(8)	99.16
V(1)–O(2)	1.867(2)	1.891	O(3)–V(1)–O(1)	98.69(8)	103.77
V(1)–O(1)	1.932(2)	1.892	O(5)–V(1)–O(1)	92.56(8)	95.37
V(1)–N(1)	2.173(2)	2.224	O(2)–V(1)–O(1)	154.51(8)	147.24
V(1)–O(4)	2.277(2)	2.492	O(3)–V(1)–N(1)	93.19(8)	92.79
Cl(1)–C(4)	1.748(2)	1.761	O(5)–V(1)–N(1)	163.26(8)	163.55
O(1)–C(1)	1.341(3)	1.331	O(2)–V(1)–N(1)	84.30(7)	81.47
O(2)–C(13)	1.326(3)	1.325	O(1)–V(1)–N(1)	77.57(7)	76.57
N(1)–C(7)	1.284(3)	1.296	O(3)–V(1)–O(4)	173.64(8)	173.21
N(1)–C(6)	1.427(3)	1.405	O(5)–V(1)–O(4)	84.52(8)	82.43
C(13)–C(8)	1.406(3)	1.422	O(2)–V(1)–O(4)	79.68(7)	73.75
C(1)–C(6)	1.399(3)	1.412	O(1)–V(1)–O(4)	79.76(7)	79.32
C(8)–C(7)	1.440(3)	1.440	N(1)–V(1)–O(4)	80.46(7)	81.98

the methanol and oxo group occupied the axial position. In this structure, vanadium has 0.290 Å distance from the main plane that is formed by O1O2O5N1. Furthermore, as can be seen from the angles in Table 3, *cis* bond angles around the V central atom are in the range between 77.57(7)° and 101.74(9)° and the range of *trans* angles varied between 154.51(8)° and 173.64(8)° which indicates that the geometry of the vanadium atom is distorted octahedrally. Comparison of the V bonds with coordinated oxygens shows that the V-O4 distance [2.277(17) Å] is longer than the others. Moreover, the V-O1 is 0.065 Å longer than V-O2, which could be attributed to the fact that O(1) is involved in hydrogen bonding .

One of the stabilization factors in the [VOL(OCH_3)($OHCH_3$)] lattice system is the hydrogen bond which is shown in Fig. 2. This bond engendered by the

interaction between O4 and O1 with a distance of 2.707 Å (Table 3) produces a dimmer structure, and, furthermore, a one-dimensional hydrogen-bonded zig-zag chain along the *b* axis is formed in the structure of cthe omplex (Fig. 3).

Table 3 Hydrogen bond for [VOL(OCH_3)($OHCH_3$)] [Å and °]

D–H···A	d(D–H)	d(H···A)	d(D···A)	<(DHA)
O(4)–H(4)···O(1)#1	0.788(18)	1.94(2)	2.707(2)	165(4)

Symmetry transformations used to generate equivalent atoms

#1 $-x + 3/2, y - 1/2, -z + 1/2$

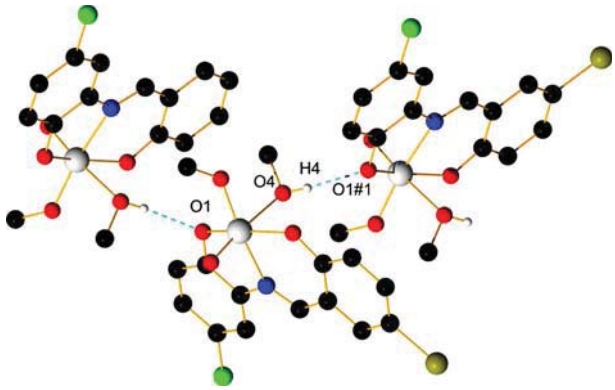

Fig. 2 Intermolecular hydrogen bonding in the complex in the solid state, *dashed blue lines*

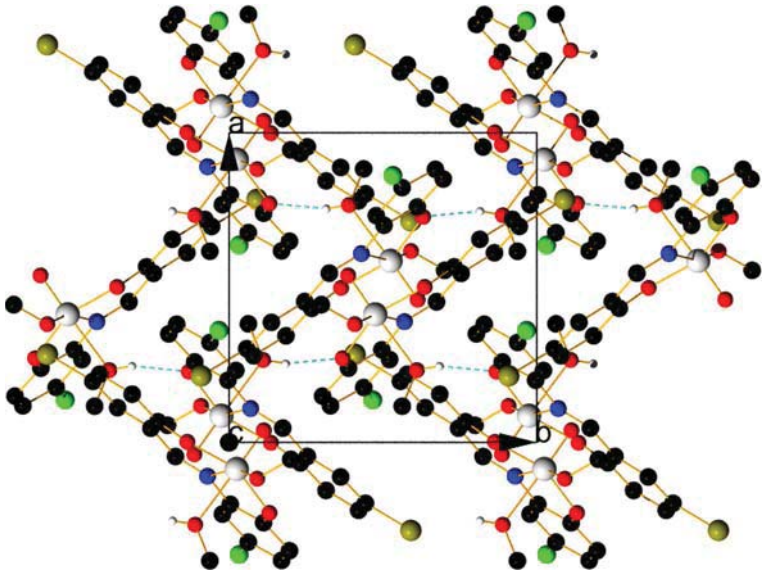

Fig. 3 Packing diagram of the complex along the *c* axis; H bonds, *dashed blue lines*

In 1971, Robinson and Gibbs introduced two parameters: [26] bond angle variance (σ^2) and mean quadratic elongation (λ). For a distorted octahedron MX_6 angle variance and quadratic elongation are defined to be:

$$\sigma^2_{\text{oct}} = \frac{1}{11}\sum_{i=1}^{12}(\theta_i - 90)^2; \quad \lambda_{\text{oct}} = \frac{1}{6}\sum_{i=1}^{6}(l_i - l_0)^2$$

Where θ_i are the X–M–X angles in the distorted octahedron, li is the length of the bond from the central M atom to the its X atom in the octahedron, and l_0 is the bond length for the ideal, regular octahedron. Similar parameters are available for the tetrahedron:

$$\sigma^2_{\text{tet}} = \frac{1}{5}\sum_{i=1}^{6}(\theta_i - 109.47)^2; \quad \lambda_{\text{tet}} = \frac{1}{4}\sum_{i=1}^{4}(l_i - l_0)^2$$

In our case, the octahedral volume of the vanadium is egal to 9.273 Å^3, the quadratic elongation is 1.040, and the angle of variance is 87.02 Å^2. This means that the octahedral coordination of the vanadium is close to the ideal octahedron, with a distortion due to the axial coordinations.

Geometry optimization, charge distributions and NBO analysis

The geometries of [$VOL(OCH_3)(OHCH_3)$] were optimized in the gas phase by the DFT method with the B3LYP function. The selected calculated geometric parameters of the complex are listed in Table 2. The calculated parameters of the complex correlate well with their resulting X-ray crystal structure data. The negligible difference between the theoretical and experimental values may originate from this fact that the experimental data belong to the solid state, while the calculated values concern single molecules in the gaseous state. The vibrational frequency calculations were performed for evidence of the accuracy of the optimized structures. The calculated atomic charges from the natural population analysis (NPA) are summarized in Table 4.

The calculated charge for vanadium is considerably lower than the formal charge (+5). In [$VOL(OCH_3)(OHCH_3)$], the central atom has an d^0 configuration, but investigating the orbital population indicates that the following data: ($d_{xy}, d_{xz}, d_{yz}, d_{x^2-y^2}, d_{z^2}$) are: 0.526, 0.618, 0.561, 0.578 and 0.743, respectively,

Table 4 Atomic charges and electron configuration from the natural population analysis (NPA)

atom	Charge	Valance arrangement
V1	1.205	[core]4S(0.23)3d(3.03)4p(0.36)
O1	−0.606	[core]2S(1.65)2p(4.95)
O2	−0.633	[core]2S(1.64)2p(4.99)
O3	−0.315	[core]2S(1.80)2p(4.50)
O4	−0.746	[core]2S(1.68)2p(5.05)
O5	−0.564	[core]2S(1.67)2p(4.89)
N1	−0.470	[core]2S(1.30)2p(4.15)

indicating significant electron donation from the donor atoms to the center metal ions. Also, all coordination sites in the ligand have a charge value and electron configuration lower than the expected amounts, so these confirm that the donations from ligand to metal are higher than the back donation.

HOMO and LUMO energy gaps indicate the stability of the compound. The molecular orbital with several of the highest HOMO and lowest LUMO contours for the complex are drawn in Fig. 4. This figure shows that the HOMO is located mainly on the ligand, but the role of ligand orbitals in LUMO reduced, and the vanadium center has a significant percentage for constructing the LUMO and higher MOs.

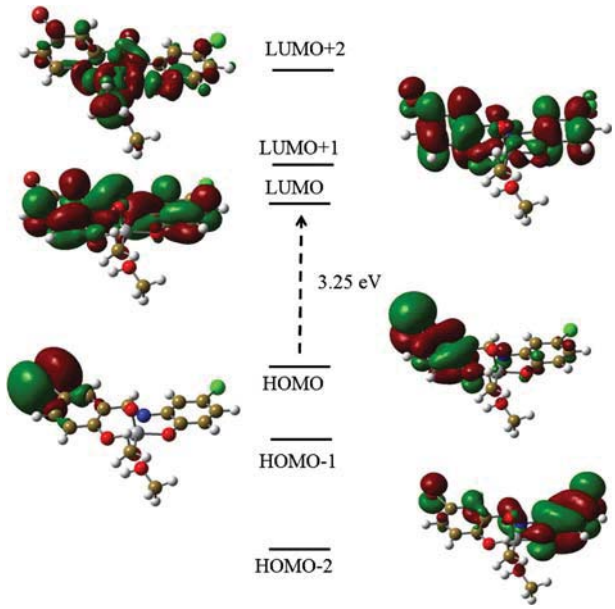

Fig. 4 Frontier molecular orbitals of the V(V) complex

Table 5 Energy and molecular orbital compositions of complex

MO	E (eV)	V (%)	L (%)	Other (%)
LUMO +4	−0.69	51	40	9
LUMO +3	−1.54	68	15	17
LUMO +2	−1.83	71	8	21
LUMO +1	−2.23	34	59	7
LUMO	−2.5	47	41	12
HOMO	−5.75	2	96	2
HOMO −1	−6.18	1	97	2
HOMO −2	−6.96	0	100	0
HOMO −3	−7.53	2	46	52
HOMO −4	−7.72	1	26	73

L deporotonated form of H_2L, *Other* OCH_3 and $OHCH_3$

Table 6 Calculated and observed IR spectrum data of oxidovanadium(V) complex

Exp.	Calc.[a]	Assignments
478 (w)	477	ν(V–N)
547 (m)	556	ν(V–O)
655 (m)	668	ν(C–Br)
709 (m)	723	ν(C–Cl)
817 (m)	826	$\delta_{opb}(C–H)_{ring}$
933 (w)	1,038	$\nu(O–C)_{alcohol}$
964 (s)	1,075	ν(V=O)
1,111 (w)	1,096	$\delta_{ipb}(CH)_{ring}$
1,297 (m)	1,308	ν(C–O)
1,357 (m)	1,341	$\nu(C=C) + \nu\ (CH)_{azomethine}$
1,525 (s)	1,510	$\nu(C=C)_{ring}$
1,604 (s)	1,602	ν(C=N)
2,942 (w)	3,011	ν_{sym}(C14)_(H)3
2,996 (w)	3,034	ν_{asym}(C14)_(H)3
3,037 (w)	3,086	ν_{sym}(C15)_(H)3
3,081 (w)	3,102	ν_{asym}(C15)_(H)3
3,082–3,159	3,161–3,223	$\nu(CH)_{ring}$
3,332 (mbr)	3,356	ν(OH)

br broad, *s* strong, *m* medium, *w* weak, *v* stretching, δ bending, *opb* out of plane, *ipb* in plane, *sym* symmetric, *asym* asymmetric

[a] Scale factor: 0.963

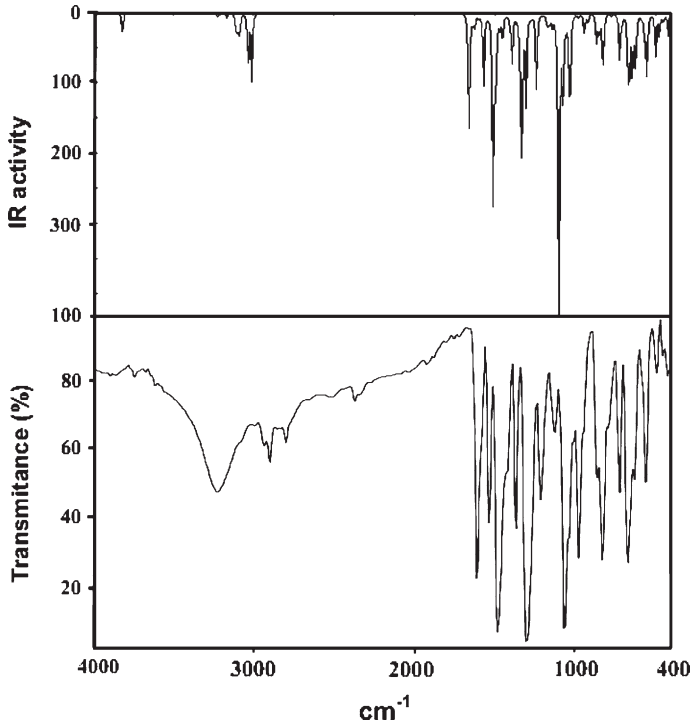

Fig. 5 Calculated and experimental FT-IR spectra for [VOL(OCH_3)($OHCH_3$)]

Details of the frontier molecular orbitals in the complex are presented in Table 5. For the complex, the LUMO is constructed from the orbitals of the ligand and the central atom while the HOMO is mainly localized on the Schiff base ligand. Based on these data, the first transition state from the HOMO to the LUMO in the complex can be assigned as an admixture of ligand–metal charge transfer (LMCT) and ligand–ligand charge transfer (LLCT).

Furthermore, some of important vibrational modes of the complex [VOL(OCH_3)($OHCH_3$)] are collected in Table 6. This molecule belongs to the C1 symmetry group. The normal modes of vibrations are distributed in the A symmetry species. In addition, the calculated and experimental vibrational spectra are given in Fig. 5.

Conclusion

A V(V) complex with the general composition [VOL(OCH_3)($OHCH_3$)] (L = tridentate ONO Schiff base) was prepared. The complex was characterized by elemental analysis, FT-IR, UV–Vis spectroscopy, and X-ray diffraction. The [VOL(OCH_3)($OHCH_3$)] complex is structurally characterized as a hexa-coordinate species with octahedral geometry in which the ligand is coordinated to the metal as tridentate bi-negatively chelating through the azomethine-*N* and two deprotonated phenolic-*O* atoms. Finally, DFT calculations in the gas phase performed on the vanadium complex produced data in good agreement with the experimental data.

Acknowledgments We thank Shahid Bahonar University of Kerman for financial assistance received. We thank Dr. Aurelien Crochet and Pr. Dr. Katharina From for the provision of a diffractometer.

References

1. G. Romanowski, M. Wera, Polyhedron **50**, 179 (2013)
2. V. Nagarajan, B. Müller, O. Storcheva, K. Köhler, A. Pöppl, Res Chem Intermed **33**, 705 (2007)
3. N.A. Lewis, F. Liu, L. Seymour, A. Magnusen, T.R. Erves, J.F. Arca, F.A. Beckford, R. Venkatraman, A. González-Sarrías, F.R. Fronczek, Eur J Inorg Chem **2012**, 664 (2012)
4. N.U. Khan, N. Pandya, N.C. Maity, M. Kumar, R.M. Patel, R.I. Kureshy, S.H.R. Abdi, S. Mishra, S. Das, H.C. Bajaj, Eur J Med Chem **46**, 5074 (2011)
5. M.R. Maurya, M. Bisht, N. Chaudhary, F. Avecilla, U. Kumar, H.-F. Hsu, Polyhedron **54**, 180 (2013)
6. J.H. McNeill, V.G. Yuen, S. Dai, C. Orvig, Mol Cell Biochem **153**, 175 (1995)
7. T.A. Clark, J.F. Deniset, C.E. Heyliger, G.N. Pierce, Heart fail. rev. 1 (2013)
8. K.H. Thompson, J. Lichter, C. LeBel, M.C. Scaife, J.H. McNeill, C. Orvig, J Inorg Biochem **103**, 554 (2009)
9. A. Bishayee, A. Waghray, M.A. Patel, M. Chatterjee, Cancer Lett **294**, 1 (2010)
10. P. Mondal, A. Hens, K.K. Rajak, Polyhedron **54**, 228 (2013)
11. A. Akbari, I. Sheikhshoaie, L. Saghatforoush, S.Y. Ebrahimipour, Z. Amiri, E-J Chem **9**(4), 2114 (2012)
12. M. Wu, H. Yu, M. Xu, Appl Catal B **129**, 351 (2013)
13. I. Sheikhshoaie, H. Stoeckli-Evans, A. Akbari, S.A. Yasrebi, S.Y. Ebrahimipour, Arab J Chem **5**, 173 (2012)
14. M.M. Islam, D. Costa, M. Calatayud, F. Tielens, J Phys Chem C **113**, 10740 (2009)
15. S.Y. Ebrahimipour, J.T. Mague, A. Akbari, R. Takjoo, J Mol Struct **1028**, 148 (2012)
16. G. Sheldrick, *SHELX-97 program for crystal structure solution and refinement* (University of Göttingen, Germany, 1997)

17. M.J. Frisch, G.W. Trucks, H.B. Schlegel, G.E. Scuseria, M.A. Robb, J.R. Cheeseman, J.A. Montgomery, T. Vreven, K.N. Kudin, J.C. Burant, J.M. Millam, S.S. Iyengar, J. Tomasi, V. Barone, B. Mennucci, M. Cossi, G. Scalmani, N. Rega, G.A. Petersson, H. Nakatsuji, M. Hada, M. Ehara, K. Toyota, R. Fukuda, J. Hasegawa, M. Ishida, T. Nakajima, Y. Honda, O. Kitao, H. Nakai, M. Klene, X. Li, J.E. Knox, H.P. Hratchian, J.B. Cross, V. Bakken, C. Adamo, J. Jaramillo, R. Gomperts, R.E. Stratmann, O. Yazyev, A.J. Austin, R. Cammi, C. Pomelli, J.W. Ochterski, P.Y. Ayala, K. Morokuma, G.A. Voth, P. Salvador, J.J. Dannenberg, V.G. Zakrzewski, S. Dapprich, A.D. Daniels, M.C. Strain, O. Farkas, D.K. Malick, A.D. Rabuck, K. Raghavachari, J.B. Foresman, J.V. Ortiz, Q. Cui, A.G. Baboul, S. Clifford, J. Cioslowski, B.B. Stefanov, G. Liu, A. Liashenko, P. Piskorz, I. Komaromi, R.L. Martin, D.J. Fox, T. Keith, A. Laham, C.Y. Peng, A. Nanayakkara, M. Challacombe, P.M.W. Gill, B. Johnson, W. Chen, M.W. Wong, C. Gonzalez, J.A. Pople, Gaussian 03, Revision C.02 (2003)
18. C. Lee, W. Yang, R.G. Parr, Development of the Colle-Salvetti correlation-energy formula into a functional of the electron density. Phys Rev B **37**, 785–789 (1988)
19. A.D. Becke, J Chem Phys **98**, 5648 (1993)
20. N.M. O'Boyle, A.L. Tenderholt, K.M. Langner, J Comput Chem **29**, 839 (2008)
21. C. Pettinari, F. Marchetti, R. Pettinari, D. Martini, A. Drozdov, S. Troyanov, Inorganica Chim Acta **325**, 103 (2001)
22. A. Rezaeifard, I. Sheikhshoaie, N. Monadi, M. Alipour, Polyhedron **29**, 2703 (2010)
23. A. Sarkar, S. Pal, Polyhedron **25**, 1689 (2006)
24. H.H. Monfared, S. Alavi, R. Bikas, M. Vahedpour, P. Mayer, Polyhedron **29**, 3355 (2010)
25. R. Dinda, P. Sengupta, S. Ghosh, T.C.W. Mak, Inorg Chem **41**, 1684 (2002)
26. K. Robinson, G. Gibbs, P. Ribbe, Science **172**, 567 (1971)